Desalination and Water Treatment
www.deswater.com

doi: 10.1080/19443994.2015.1062426

57 (2016) 14145–14157
June

Taylor & Francis
Taylor & Francis Group

Comprehensive study on interactive effects of operational parameters by using response surface method for sodium sulfate removal from magnesium stearate aqueous slurry via electrodialysis process

Mohammad Ali Masigol, Ahmad Moheb*, Arjomand Mehrabani-Zeinabad

Department of Chemical Engineering, Isfahan University of Technology, Isfahan, Iran, Tel. +98 3136500852; email: ma.masigol@gmail.com (M.A. Masigol), Tel. +98 3133915618; Fax: +98 3133912677; email: ahmad@cc.iut.ac.ir (A. Moheb), Tel. +98 3133915609; email: arjomand@cc.iut.ac.ir (A. Mehrabani-Zeinabad)

Received 30 June 2014; Accepted 6 June 2015

ABSTRACT

Detailed results of a comprehensive study on sodium sulfate removal from magnesium stearate (MgSt) aqueous slurry by using batch electrodialysis (ED) process are presented in this paper. Lowered operating costs and water consumption and avoiding from salty waste discharge to the environment were major advantageous of applying ED process in comparison with the conventional methods. The single and interactive effects of operating parameters including applied voltage, initial MgSt concentration, stirring speed, and process time on ED performance were studied by using response surface methodology method. Na recovery, specific power consumption, and sodium ion current efficiency were the objective parameters used to evaluate the ED process performance. The results showed that interaction terms of "voltage-MgSt concentration" and "stirrer speed-voltage" had the most noticeable effects on Na recovery and energy consumption, respectively. Confirmation experiments were performed at the optimum condition predicted by the model to find the response values to judge the reliability of the models. Under the optimum condition, the values obtained for Na recovery, energy consumption, and current efficiency were 73.14%, 0.523 kW h/mol, and 98.57%, respectively, which were in good agreement with the predicted values by the model.

Keywords: Response surface method; Magnesium stearate; Sodium sulfate; Batch electrodialysis; Sodium ion removal

1. Introduction

Membrane separation processes have played significant roles in many chemical processes and they are attractive alternatives for a wide range of environmental applications [1]. In recent years, electrodialysis (ED) has established itself as one of the most promising membrane technologies. ED is an electromembrane process being used for purification, desalination, and separation of ionic species in which the process driving force is an electrical field applied across a cell equipped with one or more surface-charged membrane (s) [2]. This process has been widely used for desalination of brackish and groundwater to produce drinking and process water. ED has also been utilized in wastewater treatment facilities to recover pollutant

*Corresponding author.

ions [3–6]. In addition, by using ED, desired acids/bases have been recovered from corresponding salt solutions [7–9]. Magnesium stearate (MgSt) is an additive which is frequently used as a lubricant in tablet formulation. Due to some suitable characteristics of MgSt such as low cost, chemical stability, and high melting point, it is commonly used in pharmaceutical industry [10,11]. MgSt acts as a lubricant by forming a semi-continuous film on larger excipient particles due to its very small particle size [12]. Also, MgSt is insoluble in water because of its highly non-polar molecular structure and hydrophobic nature [13].

The conventional method for MgSt production is a two-step process including two reactions described in detail elsewhere [14]. The product of the second reaction is an aqueous slurry containing MgSt and sodium sulfate (Na_2SO_4).

To produce highly pure MgSt in the dry powder form, it is essential to remove sodium sulfate from the slurry before drying the product. As a conventional method being used in Modarres Pharmaceutical and Chemical Co. (Isfahan, Iran) to remove sodium sulfate, the impure MgSt aqueous slurry goes through a multistage water scrubbing process followed by filtration at each stage. As a result, large volume of water consumption in this method reduces the economic benefits of the process.

There are large numbers of published works with the aim of ion removal [15,16] and desalination of aqueous solutions [16–19] by applying ED process. The major goal of the present work was separation of ions from an aqueous slurry with a unique nature and specific characteristics. To this aim, a three-compartment ED cell was designed and built and the effects of different operating parameters on the performance characteristics of the process were investigated. Due to the nature of the slurry and its relatively high viscosity, formation of unmixed and dead zones was possible in the feed compartment of a typical narrow and rectangular ED cell. To overcome this problem, our ED cell was designed especially with three cylindrical chambers equipped with mechanical stirrers. By implementing ED process, the contaminating sodium sulfate was removed from MgSt slurry and the ionic species (Na^+ and SO_4^{2-}) were recovered as NaOH and sulfuric acid in the cathodic and anodic compartments, respectively. The detailed results of the experiments have been reported in our previous paper [14]. The main achievement of the work was significant reduction in water consumption for purifying the produced MgSt. Also, the NaOH solution produced in the cathodic compartment could be reused in the first stage of MgSt production to synthesize sodium stearate (NaSt). Besides, the sulfuric acid formed in the anodic compartment can possibly be used to synthesize $MgSO_4$ from $MgCO_3$ or MgO. In the above mentioned work carried out by the authors, there were many operational parameters influencing the performance of the ED cell. In that work, the effect of each parameter was studied one at a time while the values of other parameters were kept constant. To optimize the process conditions, it is necessary to investigate the interactive effects of the operating parameters. Also, for the sake of process design it would be very helpful to have a mathematical model to predict the system behavior. These can be achieved by using a proper DOE method.

Response surface methodology (RSM) is a collection of statistical and mathematical techniques useful for investigating the simple effects and the interactions of operating parameters, and optimizing the processes in which an objective function of interest is affected by several variables [20]. Central composite design (CCD) is one of the methods widely used to design the experiments, which in turn is used in statistical modelings to obtain response surface models [21,22].

In the present work, the RSM was implemented to model and optimize the ED process used for MgSt purification [14]. By applying this method, it was possible to investigate the effects of independent variables, alone or in combination, on the ED performance characteristics. The optimum values of the operating variables were evaluated, and confirmation experiments were carried out to check the capability of the proposed models for predicting the responses at the optimal point.

2. Materials and methods

2.1. Membranes and solutions

The anion and cation exchange membranes used in this work were AR204SXR412 and CR67, MK111 (Ionics, MA, USA), respectively. Each membrane had an effective area of 4.0 cm × 5 cm. Principal membrane characteristics, as specified by the manufacturer, were thickness of 0.5 mm, specific weight of 13.7 mg/cm^2, water content of 46%, and bursting strength of 7 kg/cm^2. To prepare cathodic and anodic solution, proper amounts of NaOH and H_2SO_4(analytical grade, Merck, Germany) were dissolved in distilled water, respectively. Furthermore, the feed solution was prepared by dispersing proper amounts of the MgSt aqueous slurry (supplied by Modares Pharmaceutical and Chemical Co.) in deionized water.

2.2. ED setup

Fig. 1 shows a simple schematic of the three-compartment ED cell used in this study. The cell was made of polypropylene because of its proper resistance against acid and base solutions existing in the anodic and cathodic compartments, respectively, as well as its good machinery properties. Platinum coated titanium electrodes were used as anode and cathode. The surface area of each electrode was equal to 20 cm^2. Researchers usually encounter concentration polarization phenomenon and dead zone formation as two important limiting parameters during using ED processes. To overcome these problems, in this study, each chamber was stirred by a motor-driven stirrer. While the stirrers in the anodic and cathodic compartment were working at constant rate of 250 rpm, the working rate of the stirrer in the feed compartment was adjustable, varying from 0 to 600 rpm. By using an adjustable stirrer, the authors were able to investigate the influence of middle compartment stirrer speed on the ED performance. An adjustable DC power supply (Star 305, Iran) was utilized to supply voltage and direct current in the range of 0–40 V and 0–4 A, respectively, while the experiments were conducted in constant voltage mode.

2.3. Experiment design

In the present study, statistical experiment design method and RSM were implemented to model and optimize the ED process. Design expert software version 7.1.6 (STAT-EASE Inc., Minneapolis, trial version) was used to investigate the influences of four operating parameters including applied voltage (X_1), MgSt slurry concentration (X_2), feed compartment stirrer speed (X_3), and time (X_4). Extent of each variable involved five different coded levels ($\pm\alpha$ (2), ±1 and 0). The levels of the variables chosen for the design of experiments are listed in Table 1. Simultaneous interactions of the variables and their influences on the responses were studied by using three-dimensional and contour plots obtained from the software.

A regression analysis was performed to estimate the response functions as a second-order polynomial by using Eq. (1).

$$y = b_0 + \sum_{i=1}^{k} b_i x_i + \sum_{i=1}^{k} b_{ii} x_i^2 + \sum_{i<j}^{k} b_{ij} x_i x_j. \quad (1)$$

where y is the predicted response, x_i *and* x_j are the coded variables (i = 1–4 and j = 1–4), and b_0, b_i, b_{ii}, b_{ij} are the intercept, linear, quadratic, and interaction coefficients, respectively [23]. The significance and the fitness of the models were verified by using a statistical test known as analysis of variance (ANOVA) [24]. The total number of the required experiments for CCD is equal to $2^n + 2n + n_0$, including standard 2^n factorial experiments, $2n$ axial experiments on the axis at a distance of $\pm\alpha$ from the center, and n_0 replicated tests at the center of the experimental domain. It should be noted that n is the number of independent variables [21–23]. Therefore, for four variables with seven tests at the center, the number of experiments was calculated 31 ($16 + (2 \times 4) + 7 = 31$). The CCD matrix along with experimental data are given in Table 2.

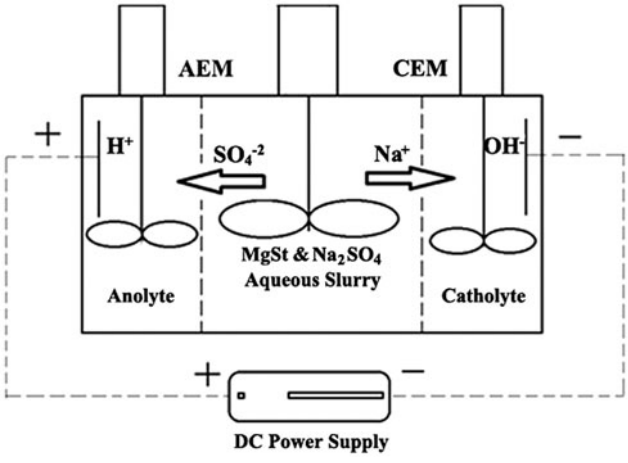

Fig. 1. Schematic diagram of the experimental ED Cell [14].

2.4. Responses determination

The responses under evaluation by RSM were sodium ion recovery (R), specific power consumption (SPC), and sodium ion current efficiency (η) which are defined by Eqs. (2)–(4), respectively. Sodium ion recovery was calculated on the basis of mole balance by using the following equation:

$$R = \frac{V_c.(C_t - C_0)}{N_f} \times 100 \quad (2)$$

In the above equation, C_0 is the initial concentration of Na^+ (mol/l) in the cathodic chamber whereas C_t denotes the sodium ion concentration at time t. Moreover, V_c is the volume of cathodic solution (l) and N_f demonstrates the initial number of Na^+ ions in the feed chamber (mol).

Table 1
Operational independent parameters

Design variables	Factor code	Actual values of coded levels				
		$-\alpha = -2$	−1	0	1	$\alpha = 2$
Voltage (V)	X_1	5	10	15	20	25
MgSt slurry concentration (wt%)	X_2	20	30	40	50	60
Stirrer speed (rpm)	X_3	200	300	400	500	600
Process time (min)	X_4	20	60	100	140	180

Table 2
Design layout using the Design Expert Version 7.1.6 software and experimental results

	Variables				Responses		
Run	X_1 (V)	X_2 (wt%)	X_3 (rpm)	X_4 (min)	Na recovery (%)	Specific power consumption (kW h/mol)	Current efficiency (%)
1	10	50	500	60	13.71	0.281	95.32
2	15	40	400	100	47.92	1.003	40.09
3	15	40	400	180	49.62	0.559	71.87
4	15	40	400	100	40.13	0.968	41.54
5	10	30	300	140	33.61	0.483	55.48
6	15	60	400	100	25.94	0.759	52.93
7	10	30	300	60	19.82	0.337	79.52
8	15	40	400	100	45.36	1.299	30.95
9	20	30	300	60	54.7	0.894	59.96
10	15	40	400	100	42.8	1.605	25.05
11	15	40	400	100	43.35	1.345	29.89
12	10	50	300	60	13.91	0.328	81.69
13	20	50	500	60	36.46	0.699	76.62
14	15	40	400	100	38.53	1.379	29.14
15	20	30	500	60	33.68	0.930	57.65
16	20	30	500	140	78.63	0.867	61.84
17	20	50	300	60	37.91	1.188	45.11
18	20	50	500	140	49.42	0.697	76.94
19	10	50	300	140	24.29	0.472	56.74
20	15	40	400	100	45.61	1.382	29.09
21	15	40	200	100	45.43	1.242	32.36
22	10	30	500	140	24.81	0.405	66.19
23	25	40	400	100	55.04	1.767	37.92
24	10	50	500	140	27.22	0.397	67.49
25	10	30	500	60	16.87	0.305	87.94
26	15	20	400	100	35.81	0.627	64.14
27	20	30	300	140	77.63	1.722	31.13
28	5	40	400	100	10.93	0.146	91.43
29	15	40	600	100	45.39	0.539	74.53
30	20	50	300	140	48.42	1.345	39.84
31	15	40	400	20	9.31	0.594	67.66

SPC can be described as the amount of energy needed for recovery of one mole of Na^+ ions from the feed solution. This parameter was defined through Eq. (3):

$$\mathrm{SPC} = \frac{E \int_0^t I(t)\ \mathrm{d}t}{N_R} \tag{3}$$

where E, I, and t are applied voltage (V), cell current (A), and operating time (s), respectively. Also, N_R represents the total moles of sodium ions (mol) which were removed from the feed compartment during the whole process time. It is worth mentioning that the required electrical power needed for stirrers was negligible in comparison with the power used for ion removal.

Sodium ion current efficiency, η (%), was determined by using the following equation:

$$\eta\,(\%) = \frac{V_c \cdot (C_t - C_0) \cdot Z.F}{\int_0^t I(t)\ \mathrm{d}t} \times 100 \tag{4}$$

where F is the Faraday constant (96,485 A s/mol) and z is the charge of the sodium ion (equal to one).

2.5. Experiment procedures

All experiments were done in batch mode. For each experiment, equal volumes (150 cm^3) of 0.5 M NaOH and 0.5 M H_2SO_4 solutions were fed into the cathodic and anodic compartments, respectively. In addition, the middle compartment was filled with the MgSt slurry with proper concentration, and stirrer speed for this compartment was adjusted according to values suggested by the DOE software for each experiment. And, finally the desired voltage was applied across the cell via the electrodes. Agitation speed in the cathodic and anodic chambers was constant at the rate of 250 rpm for all of the experiments. Each run was performed for a predetermined period of time. In order to calculate the current efficiency and SPC, cell electrical current was recorded every 15 min. At the end of each experiment, a sample of cathodic solution was taken and concentration of NaOH was determined by titration method using HCl solution and phenolphthalein as indicating agent.

3. Results and discussion

3.1. Na recovery

Coded values of the operating parameters and the results of ANOVA analysis for sodium ion recovery are reported in Table 3. By applying multiple regression analysis on the experimental data, following quadratic equation in terms of the coded factors was obtained:

$$\begin{aligned}\text{Na recovery} = {} & 43.39 + 13.78 \times X_1 - 4.51 \times X_2 - 1.23 \\ & \times X_3 + 9.07 \times X_4 - 3.53 \times X_1 \times X_2 \\ & - 0.72 \times X_1 \times X_3 + 2.86 \times X_1 \times X_4 \\ & + 2.13 \times X_2 \times X_3 - 2.64 \times X_2 \times X_4 \\ & + 1.36 \times X_3 \times X_4 - 2.22 \times X_1^2 - 2.75 \\ & \times X_2^2 + 0.88 \times X_3^2 - 3.10 \times X_4^2\end{aligned} \tag{5}$$

where X_1, X_2, X_3, and X_4 are the coded values of applied voltage, MgSt slurry concentration, feed compartment stirrer speed, and process time, respectively.

The precision of a model can be investigated by "determination coefficient (R^2)." This parameter shows the percentage of total variation results that can be explained by the suggested models. The obtained R^2 value for quadratic model of Na^+ ion recovery was equal to 0.9422, which implied that the quadratic model was well capable of representing Na^+ ion recovery under the given experimental situations. Predicted R^2 (R^2_{pred}) value (0.6992) and Adjusted R^2 (R^2_{adj}) value (0.8916) were in acceptable agreement. This concordance revealed the high accuracy of correlation between the observed and predicted values [25–28]. Fig. 2 illustrates the predicted vs. actual values for Na^+ ion recovery. Fisher's variance ratio (F-value) is defined as the ratio of the regression mean square to the error mean square and it shows how well the factors describe the variations in the data about its mean value [28,29]. The "model F-value" of 18.62 and a very low probability value (p = <0.0001), that are reported in Table 3, revealed that the model was significant. The "lack-of-fit F-value" of 4.13 implies that lack of fit is significant relative to the pure error. "Adequate precision" measures the signal-to-noise ratio which compares the range of the predicted values at the design points with the average prediction error. A quantity greater than 4 for this parameter is desirable [30]. In our study, this ratio was equal to 17.516 for Na^+ ion recovery, indicating an adequate signal-to-noise ratio. "p-values" are used as a tool to check the significance of each of the coefficients. Smaller values of P indicate more significant influence of a coefficient on the response [31,32]. Also, p-values less than 0.05 reveal that model terms are significant [33]. In this case, X_1, X_2, X_4, X_1X_2, X_2^2, X_4^2 were significant model terms.

3D response surface plots are used to investigate the relative effects of any two operating parameters while

Table 3
ANOVA of the RSM model for Na recovery

Source	Sum of square	Degree of freedom (DF)	Mean square	*F*-value	*p*-Value	Prob > *F*
Model	8,208.48	14	586.32	18.62	<0.0001	significant
X_1	4,560.35	1	4,560.35	144.84	<0.0001	
X_2	487.35	1	487.35	15.48	0.0012	
X_3	36.43	1	36.43	1.16	0.2980	
X_4	1,972.73	1	1,972.73	62.66	<0.0001	
X_1X_2	199.16	1	199.16	6.33	0.0230	
X_1X_3	8.19	1	8.19	0.26	0.6169	
X_1X_4	130.70	1	130.70	4.15	0.0585	
X_2X_3	72.46	1	72.46	2.30	0.1488	
X_2X_4	111.57	1	111.57	3.54	0.0781	
X_3X_4	29.57	1	29.57	0.94	0.3469	
X_1^2	141.39	1	141.39	4.49	0.0501	
X_2^2	216.43	1	216.43	6.87	0.0185	
X_3^2	22.28	1	22.28	0.71	0.4127	
X_4^2	275.45	1	275.45	8.75	0.0093	
Lack of fit	439.84	10	43.98	4.13	0.0482	Significant
R^2	0.9422					
Adjusted R^2	0.8916					
Predicted R^2	0.6992					
Adequate precision	17.516					

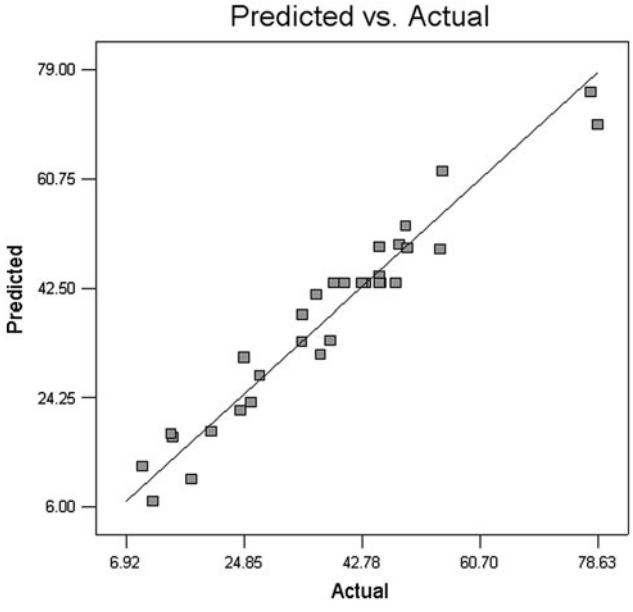

Fig. 2. Predicted vs. actual values plot for Na recovery (%).

other parameters are kept constant. As can be seen in Fig. 3(a), the Na^+ ion recovery increased almost linearly when the applied voltage increased from 10 to 25 V, irrespective of whether process time is at low or at high level. Moreover, contour plots also showed that the effect of applied voltage was more pronounced at higher process time especially after 120 min. This can be explained by the fact that increasing of voltage amplifies the electric field intensity that finally results in more driving force for ion transfer through the ED cell. In the ED process, Na^+ ion concentration gradient between the feed and cathodic compartments decreased with the passage of time; hence, the effect of applied voltage as main ED driving force is more significant at high process time values, which is observed in Fig. 3(a). Information about the interactions between MgSt slurry concentration and applied voltage are shown in Fig. 3(b). At concentrations less than 40 wt%, the applied voltage had considerable positive effects on Na^+ recovery, but for feed concentration values more than 40 wt%, the influence of voltage slightly declined. This is because of feed agglomeration at higher concentrations. This phenomenon reduces ion transfer rate, in turn leading to weakened voltage effect. ANOVA showed that the "voltage-concentration" term (X_1X_2) was the most significant in comparison with the other binary terms. Fig. 3(c) presents the 3D plot and its corresponding contour plots, showing interactive effect of feed concentration and stirrer speed on Na^+ ion recovery. This helps to draw the conclusion that stirrer speed did not affect the Na^+ ion recovery especially at feed concentrations above 40 wt%. Fig. 3(c) also shows the decrease of Na^+ ion recovery with increasing of feed

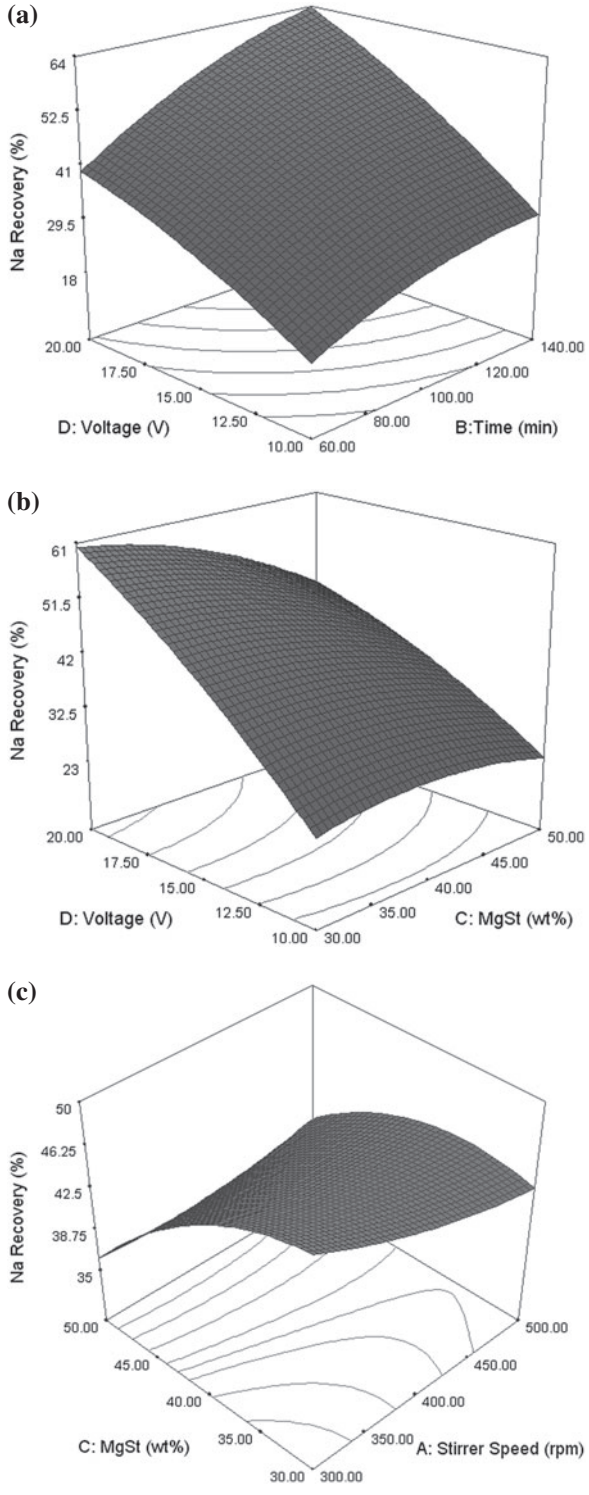

Fig. 3. Response surface plots for Na recovery. The interaction between (a) voltage and time, at fixed values of feed concentration (40 wt%) and stirrer speed (400 rpm), (b) voltage and feed concentration, at fixed values of stirrer speed (400 rpm) and time (100 min) and (c) feed concentration and stirrer speed, at fixed values of voltage (15 V) and time (100 min).

concentration for all stirrer speeds. Considering this fact, the lower levels of concentration should be chosen for maximizing the Na^+ ion recovery [14].

3.2. Specific power consumption

Based on the experimental results (Table 3), the empirical model in terms of coded factors for SPC is presented by Eq. (6).

$$\begin{aligned}\mathrm{SPC} = {} & 1.28 + 0.36 \times X_1 - 0.011 \times X_2 - 0.15 \times X_3 \\ & + 0.056 \times X_4 - 0.027 \times X_1 \times X_2 - 0.11 \times X_1 \times X_3 \\ & + 0.026 \times X_1 \times X_4 - 0.021 \times X_2 \times X_3 - 0.037 \\ & \times X_2 \times X_4 + 0.070 \times X_3 \times X_4 - 0.093 \times X_1^2 - 0.16 \\ & \times X_2^2 - 0.11 \times X_3^2 - 0.19 \times X_4^2\end{aligned} \tag{6}$$

The ANOVA results for the suggested model for SPC are given in Table 4. The model F-value of 11.14 and very low probability value ($p = <0.0001$) confirm that the obtained model is significant. R^2 was evaluated as 0.9069, and values of R^2_{adj} and R^2_{pred} were 0.8255 and 0.6726, respectively. The difference between adjusted and predicted coefficients was 0.1529 (less than 0.2). In addition, R^2 and R^2_{adj} showed a slight difference of 0.0814 (less than 0.1). These comparative values indicated a relatively high degree of agreement between the actual and predicted responses (Fig. 4). The "Lack of Fit F-value" of 0.58 implied that the Lack of Fit was not significant relative to the pure error. "Adequate precision" for the proposed model was 10.630, indicating a suitable signal-to-noise ratio. From the results reported in Table 4, two linear terms of X_1 and X_3, all the quadratic terms (X_1^2, X_2^2, X_3^2, and X_4^2), and the interaction term of X_1X_3 were significant model terms.

3D plots and their corresponding contour plots are shown in Fig. 5. Fig. 5(a) shows the influence of applied voltage and stirrer speed on the SPC at constant values of feed concentration (40 wt%) and process time (100 min). It is clear that increasing the applied voltage led to a considerable increase in energy consumption, especially at the agitation speeds less than 400 rpm. Negative effect of applied voltage on SPC was slightly reduced at speeds more than 400 rpm. To explain this effect, it should be noted that energy is generally consumed for ion transportation and water dissociation during an ED process. Also, a part of the consumed energy is dissipated as other types of energy such as heat [34]. In this case, applying higher voltages led to more energy consumption because of irreversible energy dissipation in the form of heat generation. In addition, increased cell temperature and solution vaporization were some other negative effects observed

Table 4
ANOVA of the RSM model for SPC

Source	Sum of square	Degree of freedom (DF)	Mean square	*F*-value	*p*-Value	Prob > *F*
Model	5.82	14	0. 42	11.14	<0.0001	Significant
X_1	3.06	1	3.06	82.01	<0.0001	
X_2	0.002994	1	0.002994	0.080	0.7807	
X_3	0.54	1	0.54	14.42	0.0016	
X_4	0.077	1	0.077	2.05	0.1714	
X_1X_2	0.012	1	0.012	0.31	0.5846	
X_1X_3	0.19	1	0.19	4.97	0.0404	
X_1X_4	0.011	1	0.011	0.29	0.6007	
X_2X_3	0.0068	1	0.0068	0.18	0.6753	
X_2X_4	0.022	1	0.022	0.6	0.4515	
X_3X_4	0.079	1	0.079	2.12	0.1649	
X_1^2	0.25	1	0.25	6.65	0.0202	
X_2^2	0.72	1	0.72	19.38	0.0004	
X_3^2	0.34	1	0.34	9.21	0.0079	
X_4^2	1.01	1	1.01	27.12	<0.0001	
Lack of fit	0.29	10	0.029	0.58	0.7893	Not significant
R^2	0.9069					
Adjusted R^2	0.8255					
Predicted R^2	0.6726					
Adequate precision	10.630					

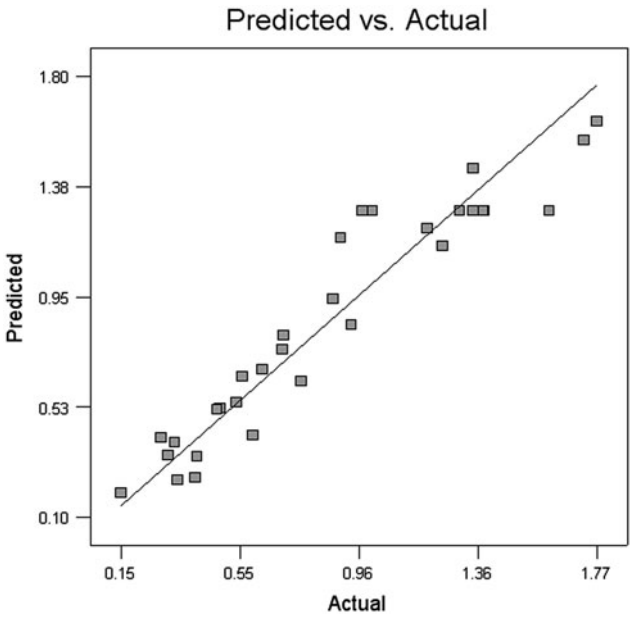

Fig. 4. Predicted vs. actual values plot for SPC.

in some preliminary tests especially at voltages higher than 25 V. As can be seen from Fig. 5(a), by applying higher stirrer speeds, less energy was consumed. This influence was more pronounced especially at higher values of applied voltage.

Fig. 5(b) represents the interaction between feed concentration and process time for fixed values of applied voltage (15 V) and stirrer speed (400 rpm). According to the results presented in Table 4, the effect of this interaction term (X_2X_4) on the energy consumption was not significant (*F*-value of 0.6 and corresponding *p*-value of $0.4515 > 0.05$). Both the feed concentration and the process time led SPC to increase when their values increased from lower level to the values in the range of 40–45 wt% and 100–120 min, respectively. For values above the mentioned ranges, the rate of increase in energy consumption was dropped. To understand this observation, it should be noted that although reduction of cell electrical resistance is usually considered as a positive impact of feed concentration increase in a typical ED process, occurrence of agglomeration for higher feed concentrations which was observed in this study was a major factor which led to reduction of ion transfer rate. As a consequence, the SPC became larger. Electrical resistance of the dilute (feed) compartment provides the major contribution to the cell total resistance. As time goes on and more ions are transferred from this compartment to the adjacent compartments, the total resistance of the cell increases and therefore energy consumption for recovery of one mole of sodium increases with the passage of time [35].

3D plot and corresponding contours of interaction between feed concentration and applied voltage (X_2X_1)

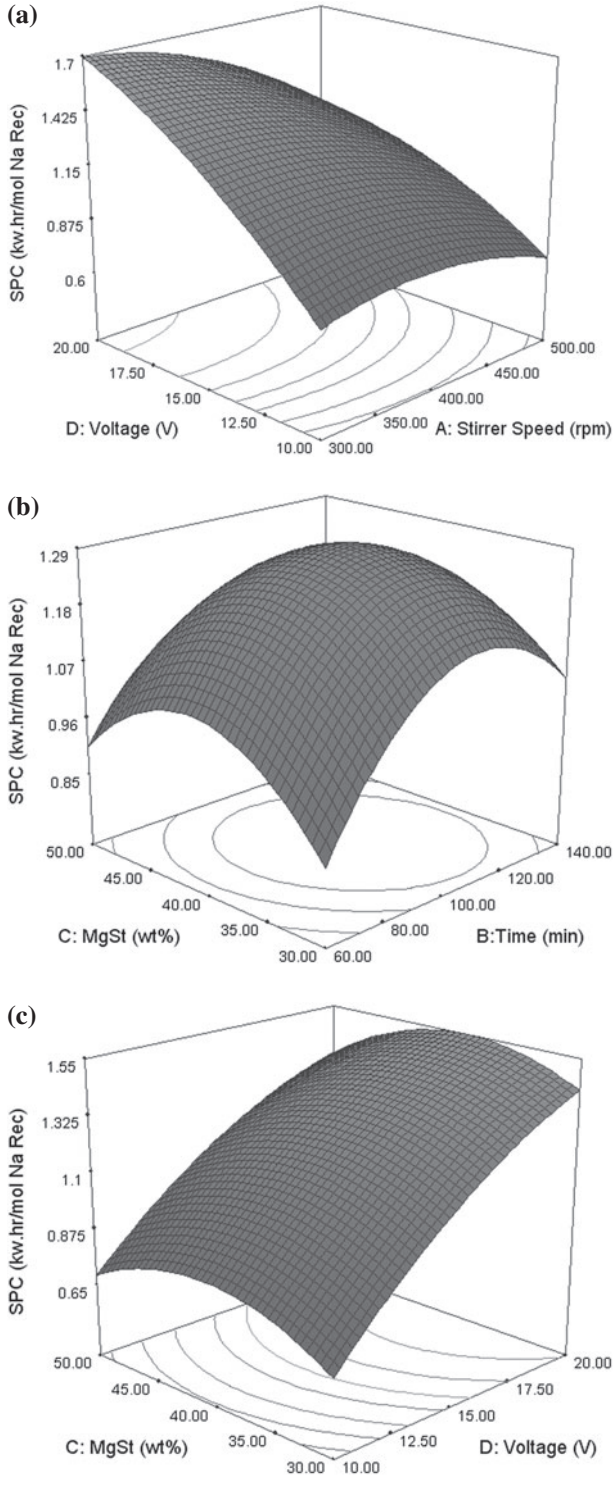

Fig. 5. Response surface plots for SPC. The interaction between (a) voltage and stirrer speed, at fixed values of feed concentration (40 wt%) and time (100 min), (b) feed concentration and time, at fixed values of stirrer speed (400 rpm) and voltage (15 V) and (c) feed concentration and voltage, at fixed values of stirrer speed (400 rpm) and time (100 min).

are shown in Fig. 5(c). As can be seen, the applied voltage had more significant influence on energy consumption in comparison with the feed concentration. Response surface contours also show that the effect of feed concentration especially at lower level of voltage was not significant. The *F*-values of the applied voltage and feed concentration presented in Table 4 (82.0 and 0.08, respectively) confirm this judgment.

3.3. Current efficiency

The performance of an ED process is usually evaluated in terms of current efficiency. This parameter is a measure of how effectively the electrical energy acts for transfer of the desired ionic species across the ion exchange membranes for a given applied current [3,35]. ANOVA was performed to verify the significance of the second-order response surface model for the current efficiency (Table 5). The "Lack of Fit *F*-value" of 2.89 implies that the Lack of Fit was not significant. R^2 with the value of 0.8991 was in agreement with the R^2_{adj} (0.8107). R^2_{pred} (0.4950) was not close enough to the R^2_{adj} (0.8107). In this case, reduction of some insignificant parameters (parameters with higher *p*-values) from the obtained model would be necessary. Hence, among the insignificant interaction terms with higher *p*-value, terms of X_2X_4 (*p*-value = 0.7308), X_1X_2 (*p*-value = 0.6686), and X_3X_4 (*p*-value = 0.3102) were removed to improve the quadratic model. The ANOVA for the reduced quadratic model for current efficiency is given in Table 6. "Model *F*-value" of 14 implied that the modified model was still significant. Also, R^2 was evaluated as 0.8902, which indicated high degree of agreement between the actual and predicted responses. Plot of actual response vs. predicted response is illustrated in Fig. 6. The value for "adequate precision" was found to be 11.264 that indicated an adequate signal-to-noise ratio. By applying multiple regression analysis on the experimental data, the modified response surface equation in terms of coded factors was obtained as the following equation:

$$\begin{aligned}\text{Current efficiency } (\%) = {} & 32.25 - 10.35 \times X_1 + 0.73 \times X_2 \\ & + 9.37 \times X_3 - 4.99 \times X_4 + 3.34 \\ & \times X_1 \times X_3 + 4.31 \times X_1 \times X_4 \\ & + 2.84 \times X_2 \times X_3 + 8.67 \times X_1^2 \\ & + 7.13 \times X_2^2 + 5.86 \times X_3^2 + 9.94 \\ & \times X_4^2 \end{aligned} \quad (7)$$

Response surface curves are plotted in Fig. 7 to understand the influences of the parameters on the sodium ion current efficiency.

Table 5
ANOVA of the RSM model for current efficiency

Source	Sum of square	Degree of freedom (DF)	Mean square	*F*-value	*p*-Value	Prob > *F*
Model	11,721.64	14	837.26	10.18	<0.0001	Significant
X_1	2,568.87	1	2,568.87	31.23	<0.0001	
X_2	12.94	1	12.94	0.16	0.6969	
X_3	2,106.75	1	2,106.75	25.61	0.0001	
X_4	597.40	1	597.40	7.26	0.0159	
X_1X_2	15.64	1	15.64	0.19	0.6686	
X_1X_3	178.89	1	178.89	2.17	0.1597	
X_1X_4	297.39	1	297.39	3.62	0.0754	
X_2X_3	129.16	1	129.16	1.57	0.2282	
X_2X_4	10.08	1	10.08	0.12	0.7308	
X_3X_4	90.35	1	90.35	1.10	0.3102	
X_1^2	2,147.75	1	2,147.75	26.11	0.0001	
X_2^2	1,454.31	1	1,454.31	17.68	0.0007	
X_3^2	981.62	1	981.62	11.93	0.0033	
X_4^2	2,824.77	1	2,824.77	34.34	<0.0001	
Lack of fit	1,089.49	10	108.95	2.89	0.1036	Not significant
R^2	0.8991					
Adjusted R^2	0.8107					
Predicted R^2	0.4950					
Adequate precision	8.985					

Table 6
ANOVA of the RSM modified model for current efficiency

Source	Sum of square	Degree of freedom (DF)	Mean square	*F*-value	*p*-Value	Prob > *F*
Model	11,605.57	11	1,055.05	14.00	<0.0001	Significant
X_1	2,568.87	1	2,568.87	34.08	<0.0001	
X_2	12.94	1	12.94	0.17	0.6833	
X_3	2,106.75	1	2,106.75	27.95	<0.0001	
X_4	597.40	1	597.40	7.93	0.0110	
X_1X_3	178.89	1	178.89	2.37	0.1399	
X_1X_4	297.39	1	297.39	3.95	0.0616	
X_2X_3	129.16	1	129.16	1.71	0.2061	
X_1^2	2,147.75	1	2,147.75	28.49	<0.0001	
X_2^2	1,454.31	1	1,454.31	19.29	0.0003	
X_3^2	981.62	1	981.62	13.02	0.0019	
X_4^2	2,824.77	1	2,824.77	37.48	<0.0001	
Lack of fit	1,205.56	13	92.74	2.46	0.1386	Not significant
R^2	0.8902					
Adjusted R^2	0.8266					
Predicted R^2	0.6033					
Adequate precision	11.264					

The combined effect of applied voltage and process time on the sodium ion current efficiency is shown in Fig. 7(a). As can be seen, by decreasing the applied voltage, current efficiency declined in almost all process time ranges studied in this work. The influence of the applied voltage on the current efficiency was more significant in comparison with process time especially at voltages less than about 16 V. Moreover,

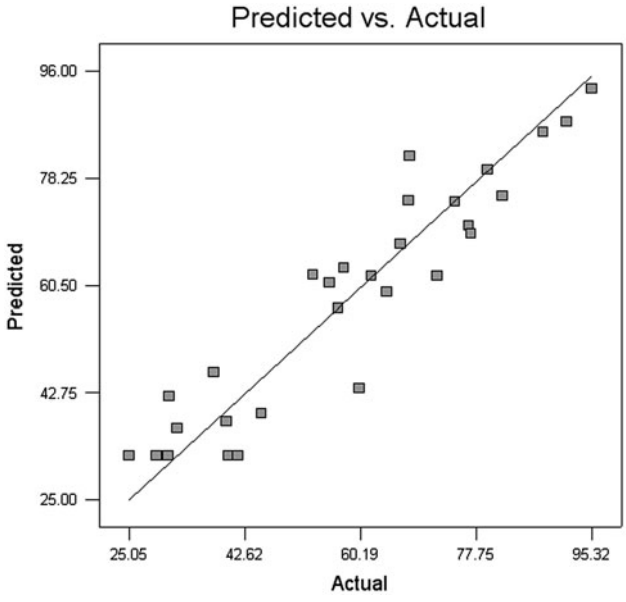

Fig. 6. Predicted vs. actual values plot for current efficiency (%).

Fig. 7(a) reveals that at the lower values of the applied voltage, process time had no significant influence on the current efficiency. A minimum point was observed for the voltage (approximately between 16 and 20 V) and the process time (approximately between 100 and 120 min). These observations can be explained by the fact that by working at higher voltages, the contribution of the applied current which is used for water dissociation and heat generation increased and therefore more energy was needed for a specific amount of ion transfer. The final result will be the reduction of current efficiency. The influence of applied voltage on current efficiency was in agreement with the findings of others such as Wu et al. [33].

It can be seen in Fig. 7(b) that the current efficiency was not significantly affected by the feed compartment stirrer speed at low applied voltage values. The positive effect of stirrer rate on the current efficiency was more pronounced especially at high voltage values. The reason was that at low voltages, the driving force was not strong enough to cause significant ion transfer between cell compartments. Therefore, increasing of feed compartment agitation speed had no noteworthy impact.

The binary effect of feed concentration and stirrer speed is shown in Fig. 7(c). It is observed that for lower stirrer speeds (<400 rpm), increasing of the feed concentration up to 40 wt% led to lowered current efficiency. This is because of agglomeration in the feed compartment which prevented ions from migrating between the feed and cathodic chambers.

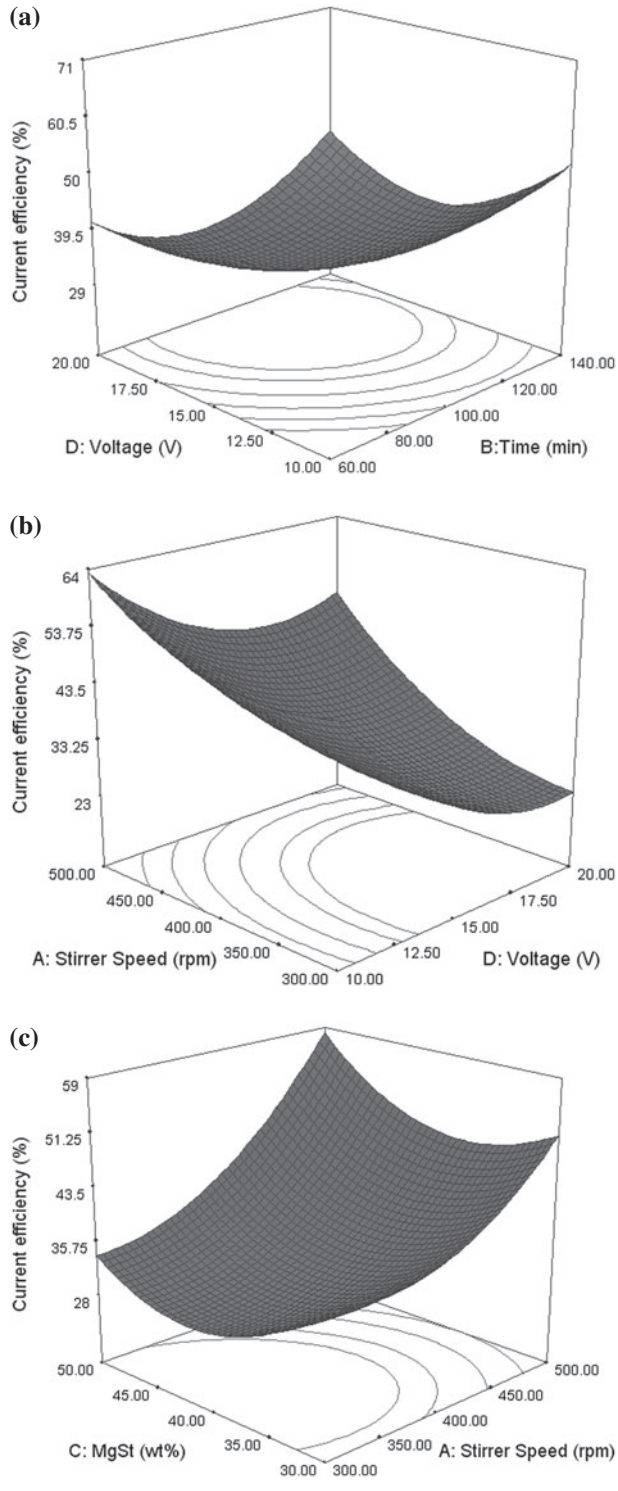

Fig. 7. Response surface plots for current efficiency. The interaction between (a) voltage and time, at fixed values of stirrer speed (400 rpm) and feed concentration (40 wt%), (b) stirrer speed and voltage, at fixed values of feed concentration (40 wt%) and time (100 min) and (c) feed concentration and stirrer speed, at fixed values of voltage (15 V) and time (100 min).

Table 7
Optimum point in terms of the actual operating variables and the output responses

Voltage (V)	MgSt concentration (wt%)	Stirrer speed (rpm)	Process time (min)	Na recovery (%)		SPC (kW h/mol)		Current efficiency (%)	
				Predicted	Actual	Predicted	Actual	Predicted	Actual
19.25	20.07	400	180	78.62	73.14	0.508	0.523	93.67	98.57

3.4. The optimization of ED process using RSM

Response surface models were used to determine the optimum values of the operating parameters. Since the Na^+ recovery and SPC were more important in comparison with current efficiency, simultaneous maximizing of Na^+ recovery and minimizing the energy consumption were the aims of optimization and the "desirability function approach" was employed for this purpose. Predicted values for the optimum conditions are reported in Table 7. To validate the adequacy of models, confirmatory tests were performed by applying the predicted optimum conditions. Results obtained from a confirmatory test are also summarized in Table 7. Formation of high turbulence in the feed compartment was usually observed when agitation speed was more than 400 rpm. To prevent this effect, stirrer rate of 400 rpm was considered as the upper limit in the optimization process. The optimized operation conditions calculated by the software were applied voltage of 19.25 V, feed concentration of 20.07 wt%, feed compartment stirrer speed of 400 rpm, and process time of 180 min. The maximum overall desirability was calculated 0.881. The obtained Na recovery was 73.14% and energy consumption was determined as 0.523 kW h/mol, both of which were in good agreement with the predicted values of the regression models (Na recovery: 78.69% and energy consumption: 0.508 kW h/mol).

4. Conclusions

In this work, the results of sodium sulfate removal from the MgSt aqueous slurry by ED process were presented. The presented paper extends our previous study [14] by investigating the interactive effects of parameters. RSM based on CCD was used to design the experiments and a set of 31 experiments were performed in order to investigate the interactions between the operational parameters including applied voltage, MgSt slurry concentration, feed compartment stirrer speed, and process time. ANOVA was utilized to check the accuracy of the response surface quadratic models. ANOVA results showed that for Na^+ recovery, interaction between voltage and MgSt concentration was the most significant parameters. Also, "voltage-stirrer rate" had more significant effect on energy consumption in comparison with other binary parameters. The optimum operating conditions were determined by the response surface models. The experimental results obtained from the confirmatory tests were in good agreement with the values predicted by the models, which in turn validated the quadratic models obtained in this work. Furthermore, it is worth mentioning that the experimental results obtained in this study show that the applied separation process has successfully achieved the goals of the work. By using the ED process, it became possible to remove a large amount of sodium sulfate from MgSt slurry and the sodium ions were recovered as sodium hydroxide. Also, it was possible to prevent generating a large amount of wastewater contaminated by sodium sulfate, which is usually produced in the conventional processes. However, it has to be admitted that the amounts of SPC were relatively high and this drawback has to be considered in further studies.

Acknowledgment

The authors would like to thank Modarres Pharmaceutical and Chemical Co. for their support in supplying raw MgSt slurry.

References

[1] R.H. Baker, Membrane Technology and Applications, second ed., John Wiley & Sons Ltd, England, 2004.
[2] H. Strathmann, Electrodialysis, a mature technology with a multitude of new applications, Desalination 264 (2010) 268–288.
[3] M. Ali, A. Mnif, B. Hamrouni, M. Dhahbi, Electrodialytic desalination of brackish water: Effect of process parameters and water characteristics, Ionics 16 (2010) 621–629.
[4] B. Jingjing, P. Changsheng, X. Huizhen, A. Abou-Shady, Removal of nitrate from groundwater using the technology of electrodialysis and electrodeionization, Desalin. Water Treat. 34 (2011) 394–401.
[5] A. Khaoua, O. Temsamani, I. Zarouf, Z. El Jalili, A. Louragli, M. Hafsi, M. El Mghari Tabib, A. Elmidaoui,

Removal of ammonium for drinking water by biological treatment and by electrodialysis, Desalin. Water Treat. 18 (2010) 157–163.
[6] C.H. Huang, T.W. Xu, Electrodialysis with bipolar membranes for sustainable development, Environ. Sci. Technol. 40 (2006) 5233–5243.
[7] S.M. Davis, G.E. Gray, P.A. Kohl, Candidate membranes for the electrochemical salt-splitting of sodium sulfate, J. Appl. Electrochem. 38 (2008) 777–783.
[8] A. Vertova, G. Aricci, S. Rondinini, R. Miglio, L. Carnelli, P. D'Olimpio, Electrodialytic recovery of light carboxylic acids from industrial aqueous wastes, J. Appl. Electrochem. 39 (2009) 2051–2059.
[9] R. Nikbakht, M. Sadrzadeh, T. Mohammadi, Effect of operating parameters on concentration of citric acid using electrodialysis, J. Food Eng. 83 (2007) 596–604.
[10] A.M. Faqih, A. Mehrotra, S.V. Hammond, F.J. Muzzio, Effect of moisture and magnesium stearate concentration on flow properties of cohesive granular materials, Int. J. Pharm. 336 (2007) 338–345.
[11] M. Perrault, F. Bertrand, J. Chaouki, An investigation of magnesium stearate mixing in a V-blender through gamma-ray detection, Powder Technol. 200 (2010) 234–245.
[12] L. Roblot-Treupel, F. Puisieux, Distribution of magnesium stearate on the surface of lubricated particles, Int. J. Pharm. 31 (1986) 131–136.
[13] P. Bracconi, C. Andrès, A. Ndiaye, Structural properties of magnesium stearate pseudopolymorphs: Effect of temperature, Int. J. Pharm. 262 (2003) 109–124.
[14] M.A. Masigol, A. Moheb, A. Mehrabani-Zeinabad, An experimental investigation into batch electrodialysis process for removal of sodium sulfate from magnesium stearate aqueous slurry, Desalination 300 (2012) 12–18.
[15] C. Gherasim, J. Křivčík, P. Mikulášek, Investigation of batch electrodialysis process for removal of lead ions from aqueous solutions, Chem. Eng. J. 256 (2014) 324–334.
[16] Z. Yu, W. Admassu, Modeling of electrodialysis of metal ion removal from pulp and paper mill process stream, Chem. Eng. Sci. 55 (2000) 4629–4641.
[17] K. Ghyselbrecht, A. Silva, B. Van der Bruggen, K. Boussu, B. Meesschaert, L. Pinoy, Desalination feasibility study of an industrial NaCl stream by bipolar membrane electrodialysis, J. Environ. Manage. 140 (2014) 69–75.
[18] T. Chakrabarty, A. Rajesh, A. Jasti, A. Thakur, A. Singh, S. Prakash, V. Kulshrestha, V.K. Shahi, Stable ion-exchange membranes for water desalination by electrodialysis, Desalination 282 (2011) 2–8.
[19] J.M. Ortiz, J.A. Sotoca, E. Expósito, F. Gallud, V. García-García, V. Montiel, A.Aldaz, Brackish water desalination by electrodialysis: batch recirculation operation modeling, J. Membr. Sci. 252 (2005) 65–75.
[20] R.A.R. Figueroa, A. Cassano, E. Drioli, Ultrafiltration of orange press liquor: Optimization for permeate flux and fouling index by response surface methodology, Sep. Purif. Technol. 80 (2011) 1–10.
[21] X.S. Yi, W.X. Shi, S.L. Yu, C. Ma, N. Sun, S. Wang, L.M. Jin, L.P. Sun, Optimization of complex conditions by response surface methodology for APAM–oil/water emulsion removal from aqua solutions using nano-sized TiO_2/Al_2O_3 PVDF ultrafiltration membrane, J. Hazard. Mater. 193 (2011) 37–44.
[22] A.L. Ahmad, S.C. Low, S.R.A. Shukor, A. Ismail, Optimization of membrane performance by thermal–mechanical stretching process using responses surface methodology (RSM), Sep. Purif. Technol. 66 (2009) 177–186.
[23] M. Khayet, C. Cojocaru, A. Baroudi, Modeling and optimization of sweeping gas membrane distillation, Desalination 287 (2012) 159–166.
[24] R.K. Goyal, N.S. Jayakumar, M.A. Hashim, A comparative study of experimental optimization and response surface optimization of Cr removal by emulsion ionic liquid membrane, J. Hazard. Mater. 195 (2011) 383–390.
[25] S. Yi, Y. Su, B. Qi, Z. Su, Y. Wan, Application of response surface methodology and central composite rotatable design in optimizing the preparation conditions of vinyltriethoxysilane modified silicalite/polydimethylsiloxane hybrid pervaporation membranes, Sep. Purif. Technol. 71 (2010) 252–262.
[26] M. Behbahani, M.R.A. Moghaddam, M. Arami, Techno-economical evaluation of fluoride removal by electrocoagulation process: Optimization through response surface methodology, Desalination 271 (2011) 209–218.
[27] N. Van Duc Long, M. Lee, Dividing wall column structure design using response surface methodology, Comput. Chem. Eng. 37 (2012) 119–124.
[28] J. Dostanić, D. Lončarević, L. Rožić, S. Petrović, D. Mijin, D.M. Jovanović, Photocatalytic degradation of azo pyridone dye: Optimization using response surface methodology, Desalin. Water Treat. 51 (2013) 2802–2812.
[29] M. Rajasimman, R. Sangeetha, Optimization of process parameters for the extraction of chromium(VI) by emulsion liquid membrane using response surface methodology, J. Hazard. Mater. 168 (2009) 291–297.
[30] M. Rajasimman, P. Karthic, Application of response surface by emulsion liquid membrane methodology for the extraction of chromium(VI), Taiwan Ind. Chem. Eng. 41 (2009) 105–110.
[31] C. Cojocaru, M. Khayet, Sweeping gas membrane distillation of sucrose aqueous solutions: Response surface modeling and optimization, Sep. Purif. Technol. 81 (2011) 12–24.
[32] K. Kishore Kumar, M. Krishna Prasad, G. Rama Lakshmi, Ch.V.R. Murthy, Studies on biosorption of cadmium on grape pomace using response surface methodology, Desalin. Water Treat. 51 (2013) 5592–5598.
[33] R.C. Wu, Y.Z. Xu, Y.Q. Song, J.A. Luo, D. Liu, A novel strategy for salts recovery from 1,3-propanediol fermentation broth by bipolar membrane electrodialysis, Sep. Purif. Technol. 83 (2011) 9–14.
[34] S.J. Parulekar, Optimal current and voltage trajectories for minimum energy consumption in batch electrodialysis, J. Membr. Sci. 148 (1998) 91–103.
[35] Z. Wang, Y. Luo, P. Yu, Recovery of organic acids from waste salt solutions derived from the manufacture of cyclohexanone by electrodialysis, J. Membr. Sci. 280 (2006) 134–137.